Title	Zn-impurity effect and interplay of s± and s++ pairings in iron-based superconductors
Author(s)	Yao, Z; Chen, W; Li, YK; Cao, GH; Jiang, H; Wang, Q; Xu, ZA; Zhang, F
Citation	Physical Review B, 2012, v. 86, p. 184515:1-184515:6
Issued Date	2012
URL	http://hdl.handle.net/10722/181707
Rights	Physical Review B. Copyright © American Physical Society.

Zn-impurity effect and interplay of $s_{\pm}$ and s_{++} pairings in iron-based superconductors

Zi-Jian Yao,[1] Wei-Qiang Chen,[1,2] Yu-ke Li,[3] Guang-han Cao,[4] Hong-Min Jiang,[1,3] Qian-En Wang,[1]
Zhu-an Xu,[4] and Fu-Chun Zhang[1,4]

[1]*Department of Physics and Center of Theoretical and Computational Physics, The University of Hong Kong, Hong Kong, China*
[2]*Department of Physics, South University of Science and Technology of China, Shenzhen 518055, China*
[3]*Department of Physics, Hangzhou Normal University, Hangzhou 310036, China*
[4]*Department of Physics, Zhejiang University, Hangzhou 310058, China*

(Received 10 September 2012; revised manuscript received 6 November 2012; published 26 November 2012)

We report theoretical and experimental studies of the effect of Zn impurity in Fe-based superconductors. Zn impurity is expected to severely suppress sign reversed $s_{\pm}$-wave pairing. The experimentally observed suppression of T_c under Zn doping strongly depends on the materials and the charge-carrier contents, which suggests competition of s_{++} and $s_{\pm}$ pairings in Fe-based superconductors. We study a model incorporating both s_{++}- and $s_{\pm}$-pairing couplings by using the Bogoliubov de-Gennes equation, and we show that the Zn impurity strongly suppresses $s_{\pm}$ pairing and may induce a transition from the $s_{\pm}$ to s_{++} wave. Our theory is consistent with various experiments on the impurity effect. We present new experimental data on the Zn-doping $SmFe_{1-x}Zn_xAsO_{0.9}F_{0.1}$ of $T_c = 50$ K, in further support of our proposal.

DOI: 10.1103/PhysRevB.86.184515 PACS number(s): 74.70.Xa, 74.20.−z, 74.62.En

I. INTRODUCTION

One of the most important issues in the high T_c Fe-based superconductors (FeSC) is their pairing symmetry.[1–3] Theories based on antiferromagnetic spin fluctuations have predicted $s_{\pm}$ pairing, where the superconducting (SC) order parameters on the hole and electron Fermi pockets have opposite signs.[4,5] The proposed symmetry is consistent with a number of experiments, such as the spin-resonance peak in neutron scattering,[6] sensitive SC junction data,[7] and quasiparticle interference in tunneling experiments.[8,9] However, the pairing symmetry in FeSC may not be universal, and there is evidence for different pairing structures as discussed in a recent review.[10]

The effect of disorder to the superconductivity is an important test to the pairing symmetry. According to Anderson's theorem, the conventional s-wave superconductivity is insensitive to nonmagnetic impurities. The sign reversed $s_{\pm}$ superconductivity is, however, sensitive to nonmagnetic impurities which scatter interband electrons. Replacement of part of Fe atoms by Co or Ni in a parent compound of FeSC leads to superconductivity. However, the role of the Co or Ni doping is more subtle and remains controversial. One scenario is that the doping introduces additional electron carriers. This scenario is supported by the angle-resolved photoemission spectroscopy, which indicates the shrinking of the hole pockets.[11] On the other hand, recent resonant photoemission spectroscopy and density-functional calculations indicate that Co doping is covalent and introduces disorder.[12] It is plausible that the Co doping introduces both carriers and disorder.[13] The Zn ion has a $3d^{10}$ configuration, hence a very high electric potential to charge carriers. Replacing an Fe atom by Zn in FeSC introduces interband scattering and is expected to severely suppress the $s_{\pm}$ superconductivity. Therefore, the Zn doping is an effective test to the $s_{\pm}$ pairing in FeSC. There have been several experiments on the Zn-doping effect on FeSC, including so-called 1111 compounds $LaFe_{1-x}Zn_xAsO_{1-y}F_y$[14,15] and more recently 122 compounds $BaFe_{2(1-x-y)}Zn_{2x}Co_{2y}As_2$ and $SrFe_{1.8-2x}Zn_{2x}Co_{0.2}As_2$.[16] The results are mixed at present, which appears to be strongly dependent on material and charge-carrier content. The experimental data on the 1111 compounds may be divided into two categories. The optimally doped $LaFeAsO_{0.9}F_{0.1}$[14] is insensitive, but the overdoped $LaFeAsO_{0.85}F_{0.15}$ is very sensitive to the Zn impurities.[15] The effect of Zn doping on Co-doped 122 compounds clearly shows the suppression of superconducting transition temperature T_c, but the reduction is much slower than the theory predicted.[16] A careful examination indicates that the suppression of T_c may be saturating at large Zn doping to some of the compounds. Note that it is not easy to dope Zn into the Fe lattices uniformly even under high pressure, and reliable data are only available up to 6% Zn doping at present. Therefore the experimental data are not complete. Nevertheless, the available experiments on Zn doping indicate complexity of the effect and suggest possible competition of sign changed $s_{\pm}$ and sign unchanged s_{++} pairings in FeSC.

In this paper, we use a two-orbital model for FeSC including both on-site-pairing (or s_{++}-pairing) coupling g_0 and next-nearest-neighbor (NNN) intersite-pairing (or $s_{\pm}$-pairing) coupling g_2 to study the Zn-impurity effect, which may help to understand the complex result of the Zn-doping effect on 1111 and 122 compounds. We apply the Bogliubov de-Gennes (BdG) equation to study the model on a finite-size system. The two SC pairings in the multiband system show interesting interplay. They may mix but also compete with each other. The disorder strongly suppresses the intersite pairing, and its effect to the superconductivity depends on the strength of g_0. For large g_0, g_2 plays little role and the pairing is s_{++} and is robust against the disorder. For small g_0, the pairing is $s_{\pm}$ and the disorder strongly suppresses superconductivity. For a moderate value of g_0, the disorder may enhance the on-site pairing and induce a transition from $s_{\pm}$ to s_{++} superconductivity. We further study the interplay between g_0 and g_2 in a clean system and show that the disorder effect on the gap functions is similar to the reduction of g_2. Our theory is consistent with the Zn-doped impurity experiments on 1111 and 122 compounds and suggests multipairing couplings in some of the FeSC. We present our new experimental data of the Zn-impurity effect

on the very high $T_c = 50$-K Sm-1111 compound. The lattice constant measurement shows that the Zn atoms are doped into the Fe lattice uniformly up to 6%. The results appear to indicate possible saturation of T_c under the Zn doping, consistent with the present theory.

II. MODEL HAMILTONIAN AND MEAN-FIELD THEORY

We consider a model Hamiltonian,

$$H = H_0 + H_{\text{pair}} + H_{\text{imp}}, \tag{1}$$

which includes a tight-binding kinetic term H_0, a pairing interaction H_{pair}, and a disordered term H_{imp}. For H_0, we consider a two-orbital model with d_{xz} (orbital 1) and d_{yz} (orbital 2) as proposed by Raghu *et al.*:[17]

$$H_0 = \sum_{\langle i\alpha, j\beta\rangle\sigma} C^\dagger_{i\sigma} \hat{h}_{ij} C_{j\sigma}, \tag{2}$$

where $C^\dagger_{i\sigma} = (c^\dagger_{i1,\sigma}, c^\dagger_{i2,\sigma})$ and $h^{\alpha,\beta}_{ij} = t^{\alpha\beta}_{i,j}$ is the electron hopping term between orbital α at site i and orbital β at site j on a two-dimensional square lattice of Fe atoms (lattice constant $a = 1$). While this model may be an oversimplified one to describe many detailed material properties of FeSC, it should capture the basic feature of the disorder effect to the pairing in systems with multi-Fermi surfaces. The nonvanishing hopping matrix elements are $t^{\alpha\alpha}_{i,i} = -\mu$, $t^{11}_{i,i+\hat{y}} = t_2$, $t^{22}_{i,i+\hat{y}} = t_1$, $t^{\alpha\alpha}_{i,i+\hat{x}+\hat{y}} = t_3$, and $t^{12}_{i,i+\hat{x}+\hat{y}} = t^{21}_{i,i+\hat{x}+\hat{y}} = -t_4$. We choose $t_1 = 1$ as the energy unit and $\mu = 1.6$, $t_2 = -1.3$, and $t_3 = t_4 = 0.85$, which gives Fermi surfaces with hole pockets near the Γ and M points and electron pockets near the X and Y points in an extended Brillouin zone as plotted in Fig. 1.

We consider randomly distributed impurities on the lattice and introduce an on-site repulsive potential on the Zn-impurity site,

$$H_{\text{imp}} = I \sum_{i\in\text{imp}} \sum_{\sigma} C^\dagger_{i\sigma} C_{i\sigma}, \tag{3}$$

where i sums over all the impurity sites, and we consider the large I case ($I = 24t_1$ in the actual calculation[18]) to model the large repulsion to an electron at the Zn site. The pairing

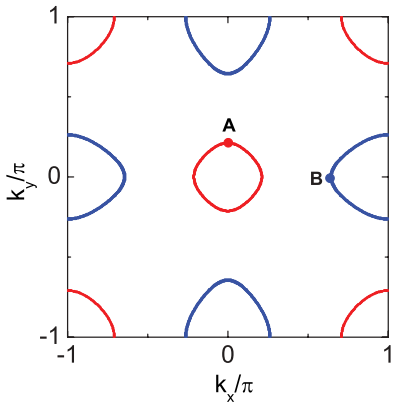

FIG. 1. (Color online) Hole (red) and electron (blue) Fermi pockets obtained in the two-orbital model Eq. (2). Points A and B are the representative $\vec{k}$ points for the hole and electron pockets, respectively.

Hamiltonian is modeled by

$$H_{\text{pair}} = -\sum_{ij,\alpha\beta} V_{ij} c^\dagger_{i\alpha\uparrow} c^\dagger_{j\beta\downarrow} c_{j\beta\downarrow} c_{i\alpha\uparrow}, \tag{4}$$

where the pairing coupling V_{ij} includes an on-site term $g_0 > 0$ and an NNN intersite term g_2:

$$V_{ij} = g_0 \delta_{i,j} + g_2 \sum_{\vec{\tau}} \delta_{i+\vec{\tau},j}. \tag{5}$$

with $\vec{\tau}$ being the vector of the two NNN site displacements. Note that the g_0 term favors s_{++} symmetry and the g_2 term favors $s_\pm$ symmetry.

We introduce a mean-field gap function $\Delta^{\alpha\alpha}_{ij} = V_{ij}\langle c_{j\alpha\downarrow} c_{i\alpha\uparrow}\rangle$. Our calculations show that the interorbital pairing Δ^{12}_{ij} (both in clean and impurity-doped systems) is very tiny, and it will be neglected below. The BdG equation for the mean-field Hamiltonian then reads

$$\sum_j \begin{pmatrix} \hat{h}_{ij} & \hat{\Delta}_{ij} \\ \hat{\Delta}^*_{ij} & -\hat{h}^*_{ij} \end{pmatrix} \begin{pmatrix} \mathbf{u}^n_{j,\sigma} \\ \mathbf{v}^n_{j,\bar{\sigma}} \end{pmatrix} = E_n \begin{pmatrix} \mathbf{u}^n_{i,\sigma} \\ \mathbf{v}^n_{i,\bar{\sigma}} \end{pmatrix}, \tag{6}$$

with $\hat{\Delta}_{ij} = \Delta_{ij}\hat{I}$ and $\hat{I}$ being an identity matrix. $\mathbf{u}_{i,\sigma} = \binom{u_{i1,\sigma}}{u_{i2,\sigma}}$. The self-consistent equation for the gap function is

$$\Delta^{\alpha\alpha}_{ij} = \frac{V_{ij}}{4} \sum_n \left(u^n_{i\alpha,\sigma} v^{n*}_{j\alpha,\bar{\sigma}} + v^{n*}_{i\alpha,\bar{\sigma}} u^n_{j\alpha,\sigma}\right) \tanh\left(\frac{E_n}{2k_B T}\right). \tag{7}$$

For the form of V_{ij} in Eq. (5), we define $\Delta^{\alpha\alpha}_0(i) = \Delta^{\alpha\alpha}_{ii}$, and $\Delta^{\alpha\alpha}_2(i) = \sum_{\vec{\tau}} \Delta^{\alpha\alpha}_{i,i+\vec{\tau}}/4$.

III. NUMERICAL RESULTS

We now discuss the numerical solutions of H. In our calculations, a 20 by 20 lattice with periodic boundary condition is used, and for each impurity content the impurity positions are randomly distributed and the statistical averages are taken over 400 times. We consider three typical cases: (i) g_0 is large and dominant; (ii) g_2 is large and g_0 is weak; and (iii) g_2 is dominant but g_0 is moderately large. In case i, the SC pairing is always s_{++} and the superconductivity is robust against the impurity as we expect from the Anderson theorem.

In Figs. 2(a) and 2(b), we show the spatially averaged on-site and NNN intersite pairing amplitudes $\Delta_0 = \frac{1}{2}\sum_\alpha \Delta^{\alpha\alpha}_0$ and $\Delta_2 = \frac{1}{2}\sum_\alpha \Delta^{\alpha\alpha}_2$ as functions of the impurity concentration n_{imp} for cases iii and ii, respectively. Also shown are the gaps at the hole pocket—point A [$(0,0.22\pi)$]—and at the electron pocket—point B [$(0.62\pi,0)$], which are the Fourier transform of the impurity averaged gaps in real space. In case ii, weak on-site pairing, the impurities strongly suppress Δ_2 as shown in Fig. 2(b). Δ_0 is tiny and the SC gap functions Δ_A and Δ_B monotonically decrease as n_{imp} increases. Because of the finite lattice size, our study is limited to the short coherence length or the strong pairing coupling cases, which require $n_{\text{imp}} \approx 0.15$ to destroy the superconductivity. We expect this value to be much smaller in weaker pairing coupling cases.

Case iii is most interesting, and our theory shows an impurity driven phase transition from $s_\pm$ to s_{++} pairings. In the absence of impurity, g_2 dominates and the pairing is $s_\pm$. As shown in Fig. 2(a), the pairing symmetry remains to be

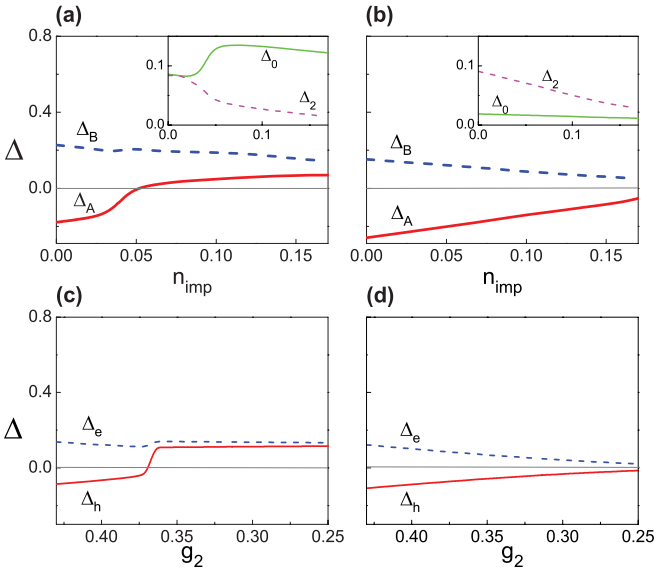

FIG. 2. (Color online) Upper panel: The gap functions Δ_A at point A of the hole pocket and Δ_B at point B of the electron pocket as functions of impurity density $n_{\rm imp}$, obtained in the mean-field solution for H. (a) For modestly strong on-site pairing coupling $g_0 = 1.8$. (b) For weak on-site coupling $g_0 = 0.8$. Insets: Spatially averaged gap functions Δ_0 (on-site) and Δ_2 (NNN intersite). In both cases, the NNN coupling $g_2 = 1.6$. Lower panel: SC gaps at electron (Δ_e) or hole pockets (Δ_h) calculated by the simplified BCS formalism, with $N_e(0) = 0.12$, $N_h(0) = 0.1$, and $\omega_D = 0.8$. (c) $g_0 = 1.8$. (d) $g_0 = 0.8$.

$s_\pm$ at $n_{\rm imp} < 0.02$, and the gap amplitudes on k points A and B are monotonically suppressed as $n_{\rm imp}$ increases. At $0.02 < n_{\rm imp} < 0.05$, $|\Delta_2|$ decreases and $|\Delta_0|$ increases. At $n_{\rm imp} > 0.05$, both Δ_A and Δ_B are positive and we have s_{++} pairing. It is interesting to note that the on-site pairing may be enhanced by the impurities due to the suppression of the NNN pairing.

We have examined the SC order parameters in real space and found that the disorder does not result in a severe pair-breaking effect to the on-site pairing measured by $\Delta_{ii}^{\alpha\alpha}$, whose peak amplitude is almost unaltered by the impurities. On the other hand, the nonmagnetic impurities not only destroy NNN SC pairing order parameter $\Delta_{i,i+\hat{x}+\hat{y}}^{\alpha\alpha}$ in larger spatial areas but also weaken the peak amplitude of the SC pairing severely.

Since the impurities suppress the NNN pairing order parameter Δ_2, this effect is similar to the reduction of g_2 in the clean sample. Therefore, tuning $n_{\rm imp}$ in the disorder system is similar to tuning g_2 in a clean system.[19] Below we shall study SC order parameters and T_c in the model Hamiltonian H as functions of g_2 in the absence of disorder to mimic the impurity effect. This enables us to further reveal the interplay between the SC pairings of s_{++} and $s_\pm$.

IV. T_c REDUCTION: THEORY AND EXPERIMENTS

For a clean system, we have lattice translational symmetry, and the gap function Eq. (7) becomes

$$\Delta_m(\mathbf{k}) = -\sum_{\mathbf{k}'} V_{mn}(\mathbf{k},\mathbf{k}')\frac{\tanh(\beta E_{n\mathbf{k}'}/2)}{2E_{n\mathbf{k}'}}\Delta_n(\mathbf{k}'), \qquad (8)$$

where m,n are the band indices, $E_{n\mathbf{k}} = \sqrt{\Delta_n(\mathbf{k})^2 + \epsilon_n(\mathbf{k})^2}$, and $\epsilon_n(\mathbf{k})$ is the single-particle energy. The summation is taken only in the vicinity of Fermi pockets with an energy cutoff ω_D. The pairing potential $V_{m,n}(\mathbf{k},\mathbf{k}')$ describes the coupling between gap functions on various Fermi pockets, and with Eq. (4) we have

$$V_{mn}(\mathbf{k},\mathbf{k}') = \sum_\alpha U_{m\alpha}(-\mathbf{k})U_{m\alpha}(\mathbf{k})U_{n\alpha}(\mathbf{k}')U_{n\alpha}(-\mathbf{k}') \times (g_0 + 4g_2\cos q_x \cos q_y), \qquad (9)$$

where m,n are band indices, α is the orbital index, $U(\mathbf{k})$ is the transformation matrix between bands and orbitals, and $\mathbf{q} = \mathbf{k} - \mathbf{k}'$ is the momentum transfer.

In our two-orbital model, there are four Fermi pockets, two for hole bands at Γ and M points, respectively, and two for electron bands at X and Y points, respectively, which makes it very difficult to solve Eq. (9) analytically. So, in the following, we will ignore the size of the pockets and assume there are four pointlike Fermi surfaces at Γ, X, Y, and M with finite densities of states. And we also assume the summation in Eq. (8) is only over the four momentum $\Gamma = (0,0)$, $Y = (\pi,0)$, $X = (0,\pi)$, and $M = (\pi,\pi)$.

Then we consider the transformation matrix under this approximation. In the two-orbital model, the two orbitals, d_{xz} and d_{yz}, mix strongly in the hole Fermi pockets. On the other hand, the two orbitals can be connected by a C_4 rotation. So, in the case of a pointlike hole Fermi surface, it is obvious that the two orbitals contribute equally to the hole pockets, i.e., $U_{h,xz(yz)}[\Gamma(M)] = \frac{1}{\sqrt{2}}$, where h denotes the hole band and xz and yz denote the two orbitals. On the other hand, the two electron pockets are dominated by the d_{xz} and d_{yz} orbital, respectively. So under the small pocket approximation, we have $U_{e,xz}(Y) = U_{e,yz}(X) = 1$ and $U_{e,yz}(Y) = U_{e,xz}(X) = 0$, and the nonzero pairing potentials are $V_{hh}(\Gamma,\Gamma) = V_{hh}(\Gamma,M) = V_{hh}(M,M) = \frac{v_0}{2}$, $V_{ee}(X,X) = V_{ee}(Y,Y) = v_0$, and $V_{he}[\Gamma(M),X(Y)] = \frac{v_2}{2}$, where $v_0 = g_0 + 4g_2$ and $v_2 = g_0 - 4g_2$.

In the small pocket approximation, the gaps on the two electron pockets should be the same because of the C_4 rotational invariance of the iron pnictide. Though the gaps on the hole pockets may be different, we still assume they are equal for simplicity. So with the above pairing potentials, we can solve the gap equation (8) and get the critical temperature:

$$k_B T_c = 1.14\omega_D e^{-1/N_h(0)\tilde{v}}, \qquad (10)$$

with $\tilde{v} = \frac{1}{2}[(1+\lambda)(g_0 + 4g_2) + \sqrt{(1+\lambda)^2(g_0+4g_2)^2 - 64\lambda g_0 g_2}]$, where $\lambda = N_e(0)/N_h(0)$ and $N_e(0)$ and $N_h(0)$ denote the density of states (DOS) at the Fermi level of electron and hole pockets, respectively.

To compare the simplified BCS theory with BdG calculations, in the lower panel of Fig. 2 we plot SC gaps as functions of g_2 with moderate [$g_0 = 1.8$, Fig. 2(c)] or weak [$g_0 = 0.8$, Fig. 2(d)] on-site pairing strength. It is seen that with moderate g_0 the pairing symmetry evolves from $s_\pm$ to s_{++} with the decreasing of g_2, while in the weak g_0 case SC gaps are monotonically suppressed with the decreasing of g_2. By comparing the upper and lower panels of Fig. 2, it is evident

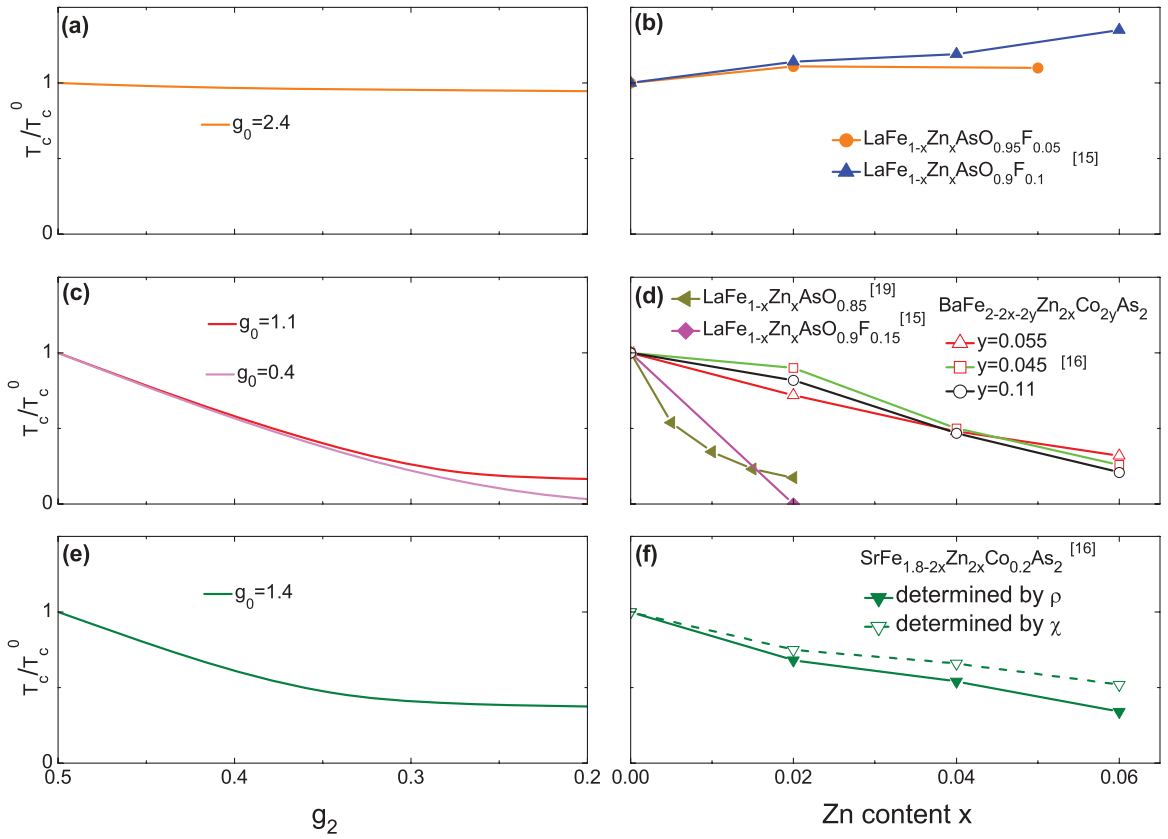

FIG. 3. (Color online) Left: The critical temperature T_c as a function of g_2 with strong, weak, and moderate on-site pairing coupling g_0. Right: Zn-impurity effect on T_c in various Fe-based superconductors observed in experiments. The references of the data are listed.

that the reduction of g_2 does qualitatively resemble the effect of Zn-impurity doping.

Our calculation on the critical temperature for various impurity concentrations, depicted in the left panel of Fig. 3, reveals that the different impurity-doping behaviors observed in FeSC[15,16] may be characterized by the strength of the effective on-site pairing potential g_0. There are three types of cases for the disorder effect. In the case of large g_0, where the on-site pairing dominates, T_c is hardly suppressed by the Zn doping. In the case of weak g_0, superconductivity is destroyed by the impurity. When g_0 is comparable with g_2, as Zn-impurity concentration increases, T_c is initially suppressed rapidly and then saturates. The experimental facts seem to support the above scenarios and the effect of Zn doping depends on the material and the charge-carrier concentration. In $LaFe_{1-x}Zn_xAsO_{0.9}F_{0.1}$ (Ref. 14), T_c are insensitive to the Zn impurity and may be explained due to large g_0. In the overdoped $LaFe_{1-x}Zn_xAsO_{0.85}F_{0.15}$ (Ref. 15) and $LaFeAsO_{0.85}$ (Ref. 20), in $BaFe_{2(1-x-y)}Zn_{2x}Co_{2y}As_2$ (Ref. 16), and in $LaFe_{1-x-y}Co_yZn_xO$ (Ref. 21), T_c decreases rapidly with the Zn doping and may belong to the category of weak g_0. In $SrFe_{1.8-2x}Zn_{2x}Co_{0.2}As_2$ (Ref. 16), T_c was found to decrease slowly and has the tendency to saturate although higher Zn doping will be needed to confirm the speculation. These scenarios are summarized in Fig. 3, which shows the critical temperature vs g_2 at different g_0 compared with the experimental data of the three types of materials that behave differently upon Zn doping.

The moderate value of the g_0 case is most interesting, for it reflects the competition between the two SC pairings. To further explore this possibility, we have prepared the $SmFe_{1-x}Zn_xAsO_{0.9}F_{0.1}$ system with $T_c = 50$ K and studied systematically the Zn-impurity effect to T_c experimentally. The results are summarized in Fig. 4. We have measured the change of the lattice constant due to Zn doping and confirmed that Zn atoms are indeed doped into the iron sites up to 6% of Zn doping [see Fig. 4(b)].[22] Beyond this doping, our data indicate that some Zn impurity may not enter into the Fe lattice so the measurement of T_c may not correspond to the uniformly doped Zn impurities. The main experimental result of T_c vs Zn concentration on this very high T_c material is plotted in Fig. 4(a). As we can see, as Zn is introduced, T_c reduces from 50 K continuously down to 40 K at 6% of Zn. The slow reduction in T_c may suggest that the superconductivity saturates at large Zn doping. It will be interesting to confirm this by doping high Zn concentration under high pressure, which remains a challenge in material preparation.

In addition to the critical temperature, another important feature during the transition from $s_\pm$ to s_{++} is the change of low-energy DOS. As shown in Fig. 5(a), the gap amplitude reduces accompanied with the increase of the low-energy DOS when the system approaches the transition point $n_{\rm imp} \approx 0.04$ from the clean limit. And if one further increases the impurity concentrations, the low-energy DOS will be suppressed again due to the reopening of the gap. The nonmonotonic behavior of DOS with impurities concentration should be able to be

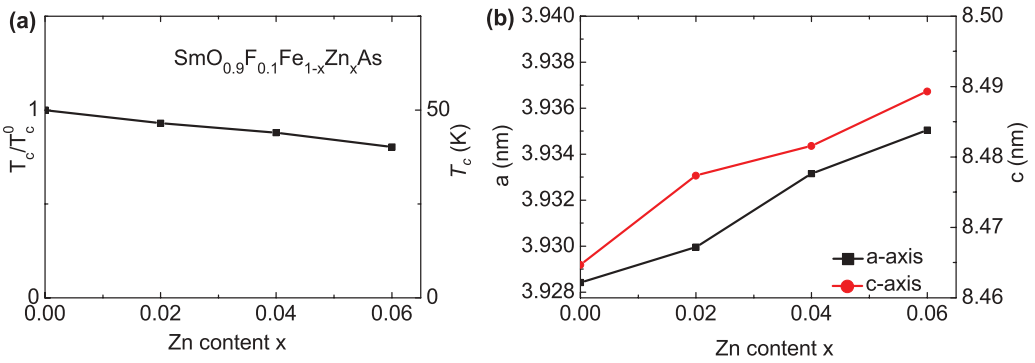

FIG. 4. (Color online) (a) T_c vs Zn-doping concentration for $SmFe_{1-x}Zn_xAsO_{0.9}F_{0.1}$. (b) Lattice constants a and c as functions of Zn-doping content in $SmFe_{1-x}Zn_xAsO_{0.9}F_{0.1}$.

directly observed by integrated photoemission spectroscopy. Meanwhile, scanning-tunneling spectroscopy, which measures the local density of states, can also be served as a probe to test our theory.

The change of DOS with impurity concentration may also be observed by other experiments which can measure the low-energy DOS, for example, the specific heat. In the superconducting state, the electron specific heat can be calculated with

$$C(T) = \frac{\partial}{\partial T}\int_{-\infty}^{\infty} EN(E)f(E)dE, \qquad (11)$$

where $N(E)$ is the DOS and $f(E)$ is the Fermi distribution function. In the low-temperature regime, the temperature dependence of the superconducting order parameter is very weak and can be neglected. So we use the zero-temperature DOS to calculate the specific heat with Eq. (11). In order to relate our calculations with the experiments directly, we use $\Delta_{\rm coh} \approx 0.18t_1 = 6$ meV as the energy scale, and the result is depicted in Fig. 5. We find that the electron specific heat below 10 K is small in the clean limit and shows a significant increase with approaching the transition point by increasing impurity concentrations. When the system is stabilized in the s_{++} state, $C(T)$ drops to a low value again, and the absolute value shown in Fig. 5(b) is in the same order or even larger than the experimental measurement of 1111 material.[23] So it should be able to be observed in experiments.

We note the recent work of Efremov *et al.*,[24] who applied the T-matrix method to study the nonmagnetic effect on FeSC. Our microscopic theory shares some similarities with theirs. In their phenomenological theory the impurity-doping behavior is found to be associated with the averaged pairing coupling strength. In our theory, the decisive role of on-site pairing on the impurity effect is identified. It is also worth mentioning that, based on the mechanism of orbital-fluctuation-mediated superconductivity, Kontani *et al.*[25] obtained a similar crossover from the $s_{\pm}$ state to the s_{++} state upon impurity doping.

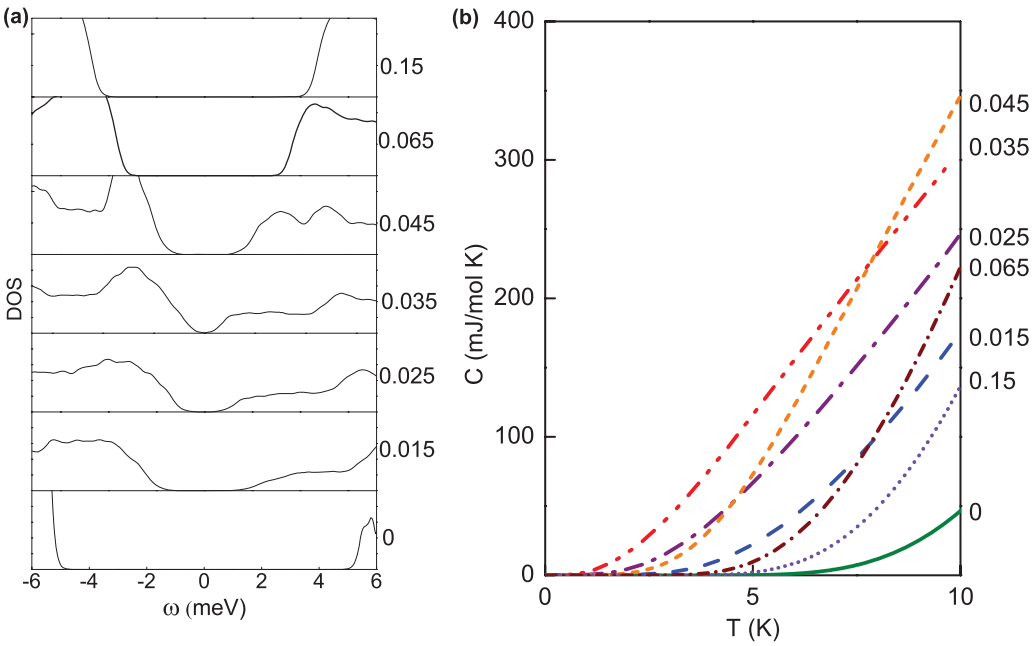

FIG. 5. (Color online) (a) DOS for various impurity concentrations. $n_{\rm imp} = 0,0.015,0.025,0.035,0.045,0.065$, and 0.15 from bottom to top. (b) The low-temperature specific heat at various impurity concentrations.

V. SUMMARY

In summary, we have studied the disorder-induced pair-breaking effect on the Fe-based superconductors using a model that incorporates both the on-site and NNN pairings. We show that the Zn impurity largely suppresses NNN pairing. Its effect to the superconductivity depends strongly on the on-site pairing coupling strength g_0. The superconductivity can be robust, or evolves a transition from $s_\pm$ to s_{++}, or is strongly suppressed in the presence of the disorder. Our theory qualitatively explains different reductions of T_c in various iron pnictide superconductors observed in the experiments on the Zn-impurity effect. We also predict the possible Zn-impurity doping induced transition from $s_\pm$- to s_{++}-pairing states in certain samples. Furthermore, we have systematically prepared Sm-1111 samples with $T_c = 50$ K under the Zn doping and show that the reduction of T_c could be consistent with the scenario of a moderate on-site s-wave pairing. It will be highly interesting and important to prepare systematic controlled samples with higher Zn doping to experimentally confirm or falsify the theory. The reduction of the gap in DOS during the transition from $s_\pm$ to s_{++} can be observed by integrated photoemission spectroscopy or specific-heat experiments. Finally we remark that the explicit pairing forms are unlikely to be universal in Fe-based superconductors, in contrast to the universal d-wave pairing in cuprates.

ACKNOWLEDGMENTS

This work is partly supported by Hong Kong Research Grants Council (RGC) Grant No. 10931160425 and NSFC/RGC Joint Research Scheme Grant No. N_HKU 726/09.

[1] H. Ding *et al.*, Europhys. Lett. **83**, 47001 (2008).
[2] T. Sato *et al.*, Phys. Rev. Lett. **103**, 047002 (2009).
[3] C. Liu *et al.*, Phys. Rev. Lett. **101**, 177005 (2008).
[4] I. I. Mazin, D. J. Singh, M. D. Johannes, and M. H. Du, Phys. Rev. Lett. **101**, 057003 (2008).
[5] F. Wang, H. Zhai, Y. Ran, A. Vishwanath, and D.-H. Lee, Phys. Rev. Lett. **102**, 047005 (2009).
[6] A. D. Christianson *et al.*, Nature (London) **456**, 930 (2008).
[7] C.-T. Chen, C. C. Tsuei, M. B. Ketchen, Z.-A. Ren, and Z. X. Zhao, Nature Physics **6**, 260 (2010).
[8] M. L. Teague, G. K. Drayna, G. P. Lockhart, P. Cheng, B. Shen, H.-H. Wen, and N.-C. Yeh, Phys. Rev. Lett. **106**, 087004 (2011).
[9] T. Hanaguri, S. Niitaka, K. Kuroki, and H. Takagi, Science **328**, 474 (2010).
[10] P. J. Hirschfeld, M. M. Korshunov, and I. I. Mazin, Rep. Prog. Phys. **74**, 124508 (2011).
[11] C. Liu *et al.*, Nature Physics **6**, 419 (2010).
[12] G. Levy *et al.*, Phys. Rev. Lett. **109**, 077001 (2012).
[13] T. Berlijn, C.-H. Lin, W. Garber, and W. Ku, Phys. Rev. Lett. **108**, 207003 (2012).
[14] Y. Li, X. Lin, Q. Tao, C. Wang, T. Zhou, L. Li, Q. Wang, M. He, G. Cao, and Z. Xu, New J. Phys. **11**, 053008 (2009).
[15] Y. Li, J. Tong, Q. Tao, C. Feng, G. Cao, W. Chen, F. chun Zhang, and Z. an Xu, New J. Phys. **12**, 083008 (2010).
[16] J. Li, Y. Guo, S. Zhang, Y. Tsujimoto, X. Wang, C. Sathish, S. Yu, K. Yamaura, and E. Takayama-Muromachi, Solid State Commun. **152**, 671 (2012).
[17] S. Raghu, X.-L. Qi, C.-X. Liu, D. J. Scalapino, and S.-C. Zhang, Phys. Rev. B **77**, 220503 (2008).
[18] We have checked using several values of I, the main conclusion is not sensitive to the precise value of I as long as I is large.
[19] The impurity also slightly affects the on-site pairing gap.
[20] Y. F. Guo *et al.*, Phys. Rev. B **82**, 054506 (2010).
[21] Y. Li *et al.* (unpublished).
[22] As seen in Fig. 4(b), the lattice constant a decreases slightly with the Zn doping, while c increases obviously. As a result, the cell volume of LaFeZnOF increases monotonously with increasing Zn content. Note that the lattice constant of LaOZnAs is larger than that of LaOFeAs [see André T. Nientiedt and Wolfgang Jeitschko, Inorg. Chem. **37**, 386 (1998)]. The energy-dispersive x-ray spectrometry analysis measurement shows that the actual Zn content in these samples is very consistent with the nominal composition, which suggests that Zn impurities should be successfully doped into the lattice.
[23] G. Mu, H. Luo, Z. Wang, L. Shan, C. Ren, and H.-H. Wen, Phys. Rev. B **79**, 174501 (2009).
[24] D. Efremov, M. Korshunov, O. Dolgov, A. Golubov, and P. Hirschfeld, Phys. Rev. B **84**, 180512(R) (2011).
[25] H. Kontani and S. Onari, Phys. Rev. Lett. **104**, 157001 (2010).